AFFDL-TR-68-150

SOME APPLICATIONS OF FINITE ELEMENT ANALYSIS TO SHELL BUCKLING PREDICTION

Walter E. Backus* Raymond M. Mello**

The Boeing Company Seattle, Washington

The application of the direct stiffness method in the solution of doubly curved shell stability problems is demonstrated. Discussed first are the modifications necessary to the basic linear matrix displacement approach of structural analysis to solve large deflection and stability problems. The resulting nonlinear system of equations is solved using the piecewise linearization technique. Buckling loads are predicted for several shallow spherical shells of varying geometry and compared to known solutions. Finally, the method is applied to a radome shell with nonuniform surface loads and the critical buckling load is established.

* Research Specialist, Missile and Information Systems Division, Structures and Materials Technology

** Research Engineer, Missile and Information Systems Division, Structures and Materials Technology

SECTION I

INTRODUCTION

Historically, the analysis of doubly curved shells may be traced back to 1912 when Hans Reissner (Reference 1) presented the governing equations for symmetrically loaded spherical shells of constant thickness. These equations were quite unwieldy, but by assuming very thin shells, A. Van der Neut (Reference 2) obtained the classical solution for buckling of spheres. Since these original publications, a sizable effort has been extended in the stability analyses of doubly curved shells by many prominent people using the classical or differential equation method. However, much of the work has been restricted to thin shells with uniform loadings because of the degree of mathematical tractability of the problem. Extensive data has been generated (References 3, 4, and 5) that indicate buckling strength of uniformly loaded cylinders, spheres, cones, and plates. However, for other shell geometries there are few sources available, and if the loading is anything other than uniform pressure there is essentially no buckling data.

As an example of the difficulty encountered in the buckling analysis of thin shells, the buckling analysis of shallow spherical caps first appeared in 1939 (Reference 6); since that time it has been studied by approximately 25 investigators and has only recently yielded a solution (Reference 7) that essentially agrees with test data. Hence, it appears that an alternate approach for analysis of less simple shell problems that we commonly encounter in the aerospace industry must be found. In our particular case, we were interested in the buckling analysis of a large proposed radome shell (Figure 1) with unsymmetrical loading to be mounted on an aircraft, for which no solution could be found in the appropriate literature. In this paper, the alternative scheme being proposed to predict the behavior of irregularly shaped and loaded doubly curved shells is the direct stiffness approach. In this method, the continuous shell structure is replaced by a system of structural or finite elements that are interconnected at a discrete number of nodal points or joints. Because each element can be considered as a separate unit, different material properties, thicknesses, and nonuniform loadings can be ascribed to the different elements. The primary basis of this method of analysis is a relationship between nodal force quantities and their corresponding displacement quantities. Such a relationship is called the stiffness of the finite element.

Practical finite element analysis of structures dates from 1954 to 1956 when three treatises (References 8, 9, and 10) were published on the subject and these analysis procedures have received general acceptance in the analysis of complex structures. These original

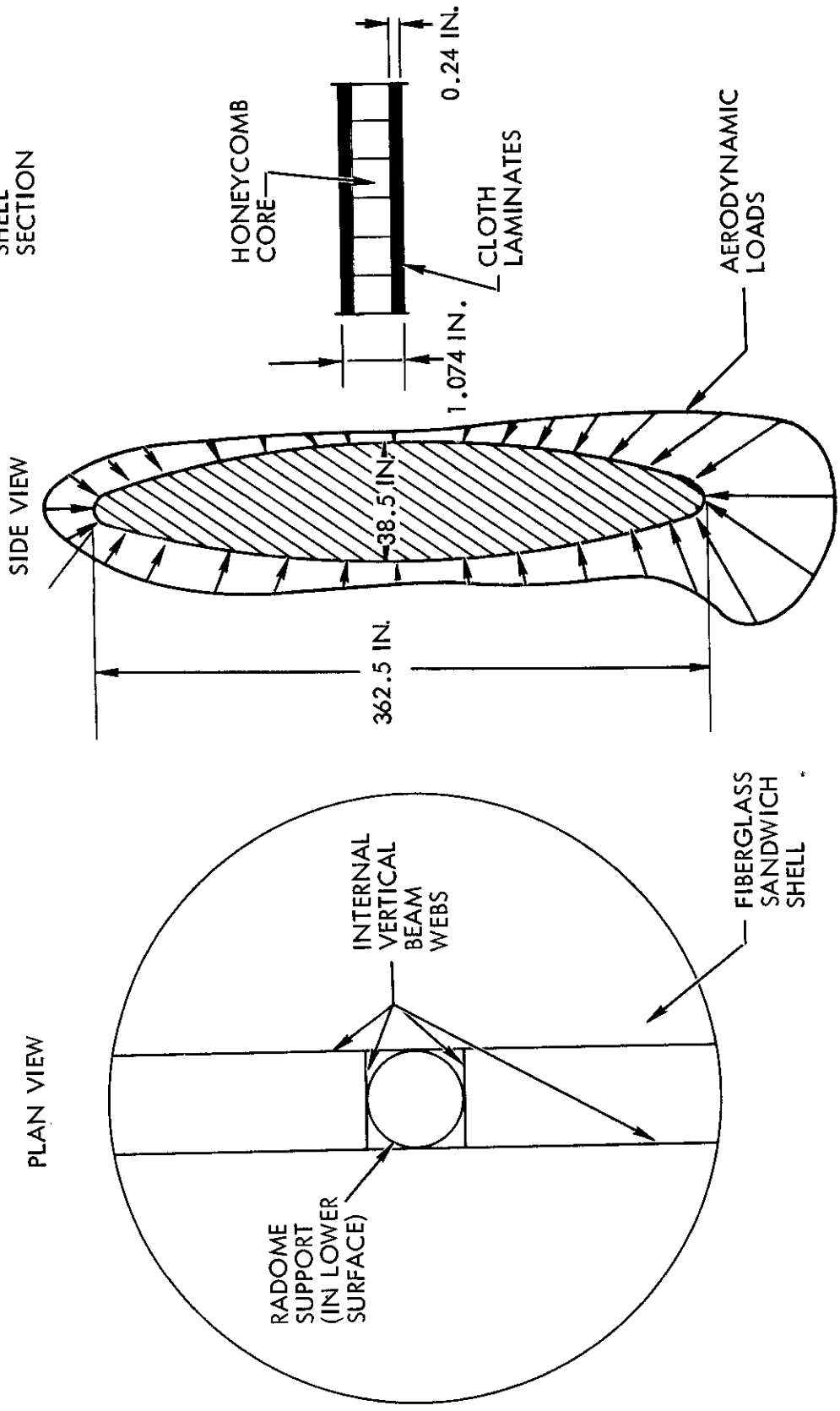

Figure 1. Radome Shell Structure

proposed analytic procedures were only applicable to linear structural analyses and only recently has much attention been devoted to the development of finite element techniques to handle nonlinear problems such as instability analyses and large deflection analyses. Expansion of the stiffness method to handle nonlinear, large deflection problems was first proposed by M.J. Turner, et al., in 1960 (Reference 11). Turner, et al., in 1962 (Reference 30) enlarged on the nonlinear finite element technique to an eigenvalue procedure to determine the buckling strength of columns. Using a similar procedure, although not identical, Gallagher and Padlog (Reference 31) derived a stability coefficient matrix to predict column buckling. Next, R. H. Gallagher, et al., (Reference 12) applied a finite element procedure to obtain instability temperature of a heated restrained bar. In his procedure, the lowest eigenvalue of the initial stiffness matrix is determined to define the instability load. B. J. Hartz, independently at the University of Washington, derived the stability coefficient matrices for columns (Reference 13) and flat plates (Reference 14) to predict buckling loads using the finite element method. H. C. Martin (Reference 15), of The Boeing Company, applied the piecewise linearization (incremental load) technique first suggested in Reference 11 to the buckling analysis of a plate and tapered column. Also. R. H. Gallagher, et al., (Reference 16) has extended his technique (Reference 12) to determine the buckling strength of a shallow spherical shell. The finite element technique used in this paper to determine the buckling load of a doubly curved shell is an extension of H. C. Martin's (Reference 15) procedure to shells and has been developed over a number of years at The Boeing Company. In this procedure, the load is applied to the structure in increments and the stiffness is updated for each increment. All nodal freedoms, except those expected to be in the buckle, can be reduced out of the stiffness matrix so that the matrix can be inverted "in core" in current computers even though several hundred nodes may be required to define the structure adequately. Buckling is indicated when the stiffness matrix becomes nonpositive definite.

Our main concern for instigating this study and paper was the requirement to analyze a monocoque radome shell in which the unsymmetrical design loads caused large membrane compression stress in areas where the aerodynamic pressure was high. Because direct verification of the analysis procedures by test of a radome could not be funded, we decided first to apply this piece-wise linearized finite element technique to shallow spherical caps where considerable theoretical and test data was available (Figure 2). Though many conflicting theoretical solutions are shown in Figure 2 it appears that the curve shown in Figure 2d is the best basis for comparison. Hence, the bulk of this paper is concerned with the analysis of the shallow shell. The effect on shallow shell results due to variation in element size and incremental load size were investigated so that economical sizes could be selected for the radome analysis. After we had determined the correlation between finite element results and more exact solutions for the shallow shell, we then applied the procedure to the radome analysis.

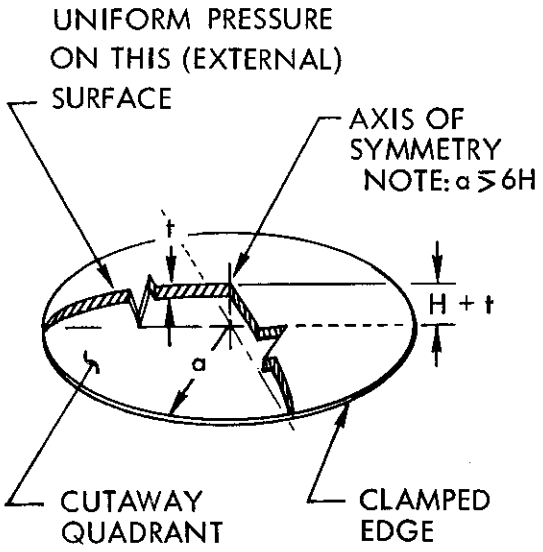

a. CLAMPED SHALLOW SPHERICAL SHELL LOADED BY UNIFORM EXTERNAL PRESSURE

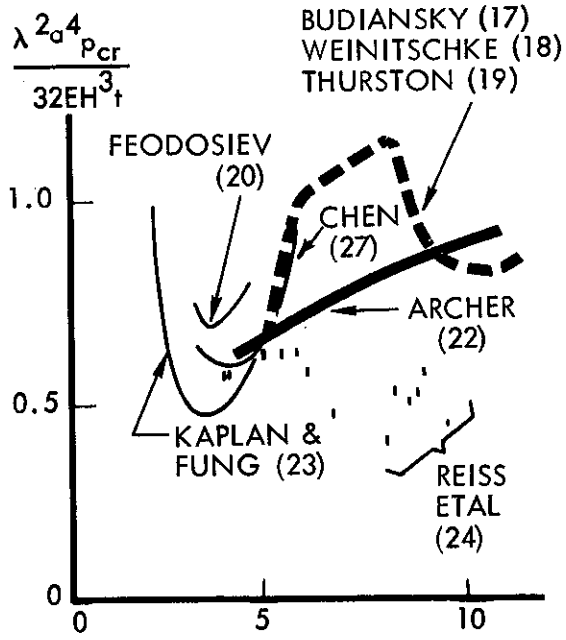

$$\lambda = 2\left[3(1-\nu^2)\right]^{1/4}\sqrt{H/t}$$

b. SYMMETRIC SOLUTIONS

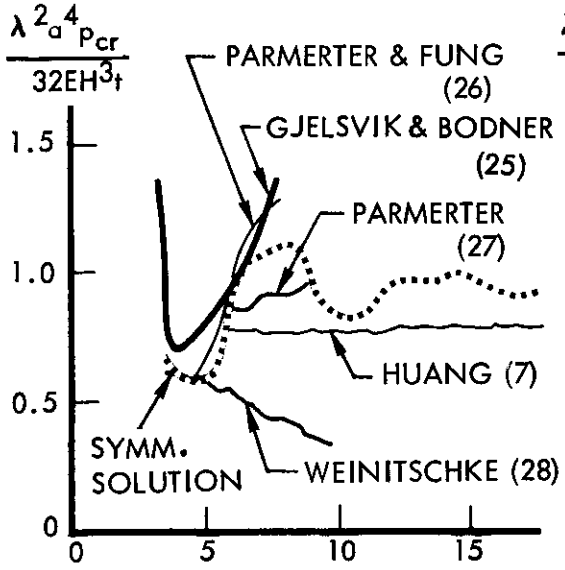

$$\lambda = 2\left[3(1-\nu^2)\right]^{1/4}\sqrt{H/t}$$

c. ASYMMETRIC SOLUTIONS

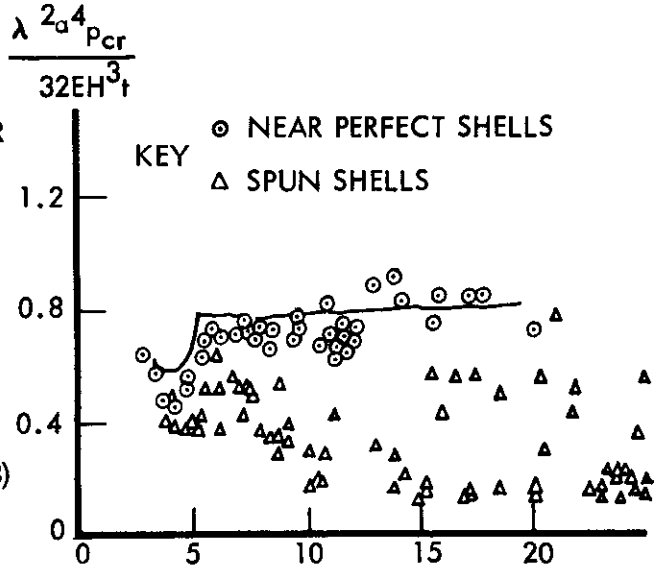

$$\lambda = 2\left[3(1-\nu^2)\right]^{1/4}\sqrt{H/t}$$

d. EXPERIMENTAL DATA

Figure 2. Buckling Data--Shallow Spherical Shells

SECTION II

THEORETICAL CONSIDERATIONS

LINEAR ANALYSIS

The basic idea of the finite element technique of structural analysis resides in the physical idealization of a structure as an assemblage of structural elements such as bars, beams, plates, and shell elements. These elements are connected to each other at discrete points called nodes and the assemblage of the finite elements is termed "the structural idealization of the real structure."

Having replaced the real structure by an idealized one, the analysis of the structure reduces to the purely mathematical problem of determining the distribution of load among elements of known elastic properties. This analysis is carried out in two steps. First, for each discrete element, a linear relationship is determined between the element corner or ends (node) forces and deformations of the form

$$Q = kq \quad \text{(Force - displacement or "stiffness" equations)} \tag{1}$$

where

Q = matrix of forces applied to element nodes

k = element stiffness matrix

q = matrix of associated deflections at the element nodes

using an assumed displacement distribution. Once the element relationships have been determined, the complete analysis of the structure reduces to a systematic combination of individual unassembled structural elements into an assembled structure in which the conditions of equilibrium and continuity are satisfied at the nodes and along element boundaries. Although it is convenient to visualize the finite elements as being connected to each other at the nodal points, this does not imply that discontinuities are permitted along element boundaries between nodes. Displacement functions representing the elements are chosen so that continuity is achieved along element boundaries. In some cases this continuity may be violated when distinctly different types of elements are used in representing the real structure.

The governing equation of the complete structure takes the form

$$R = Kr \tag{2}$$

where

$\mathbf{R}$ = matrix of external forces of the structure applied at the nodes

$\mathbf{K}$ = gross stiffness matrix or structure stiffness matrix

$\mathbf{r}$ = matrix of associated deflections or freedoms at the nodes

There are two procedures commonly used to form the gross stiffness matrix. The first procedure uses a geometric relationship between the element nodes and the generalized displacements or freedoms of the structure of the form

$$\mathbf{q} = \mathbf{a}\,\mathbf{r} \tag{3}$$

where $\mathbf{a}$ is a coordinate transformation matrix. Using the above transformation matrix, the elemental stiffness matrices are modified and added to form a gross stiffness matrix

$$\mathbf{K} = \mathbf{a}^{T}\,\mathbf{k}\,\mathbf{a} \tag{4}$$

for the complete structure.

A more direct procedure, labeled the direct stiffness method, that is especially useful for large problems can be carried out automatically by the digital computer. By choosing the generalized displacements to be displacements of the corners or nodes of each element, the elements of the $\mathbf{a}$ matrix will be either zero or unity. It follows that the stiffness matrix $\mathbf{K}$ for the complete structure can be formed by the implied summation of the elemental stiffness coefficients.

Once the stiffness matrix has been obtained, the displacement boundary conditions can be applied to at least eliminate rigid-body motions, reducing the stiffness matrix and causing it to be positive definite. The solution for the displacements thus may be obtained by inverting the stiffness matrix to form the flexibility matrix or

$$\mathbf{r} = \mathbf{K}^{-1}\,\mathbf{R} \tag{5}$$

Internal stresses can also be found now because the nodal displacements define the deformed state of each element.

EXTENSION TO GEOMETRICALLY NONLINEAR PROBLEMS

To apply the direct stiffness method to geometrically nonlinear problems such as large deflection and stability analyses, the stiffness equation must be modified. For a nonlinear

problem, the stiffness matrix $\mathbf{K}$ is a function of displacements $\mathbf{r}$ and the stiffness equation may be written as follows

$$\mathbf{K}(\mathbf{r})\,\mathbf{r} = \mathbf{R} \tag{6}$$

To solve these nonlinear equations, the piecewise linearization is applied. To the load $\mathbf{R}$ in Equation 6, an incremental load variation $\Delta\mathbf{R}$ is applied for which $\mathbf{r}$ will have a variation $\delta\mathbf{r}$. Therefore, Equation 6 becomes

$$\left[\mathbf{K}(\mathbf{r}+\delta\mathbf{r})\right]\left[\mathbf{r}+\delta\mathbf{r}\right] = \left[\mathbf{R}+\Delta\mathbf{R}\right] \tag{7}$$

Substituting the following approximation into Equation 7 and expanding

$$\left[\mathbf{K}(\mathbf{r}+\delta\mathbf{r})\right] = \left[\mathbf{K}(\mathbf{r})\right] + \left[\delta\mathbf{K}(\mathbf{r},\delta\mathbf{r})\right] \tag{8}$$

Equation 7 becomes

$$\left[\mathbf{K}(\mathbf{r})\right]\left[\mathbf{r}\right] + \left[\mathbf{K}(\mathbf{r})\right]\left[\delta\mathbf{r}\right] + \left[\delta\mathbf{K}(\mathbf{r},\delta\mathbf{r})\right]\left[\mathbf{r}\right] + \left[\delta\mathbf{K}(\mathbf{r},\delta\mathbf{r})\right]\left[\delta\mathbf{r}\right] = \left[\mathbf{R}+\Delta\mathbf{R}\right] \tag{9}$$

Subtracting Equation 6 from this above equation, we arrive at the incremental stiffness equation

$$\left[\mathbf{K}(\mathbf{r})\right]\left[\delta\mathbf{r}\right] + \left[\delta\mathbf{K}(\mathbf{r},\delta\mathbf{r})\right]\left[\mathbf{r}\right] + \left[\delta\mathbf{K}(\mathbf{r},\delta\mathbf{r})\right]\left[\delta\mathbf{r}\right] = \left[\Delta\mathbf{R}\right] \tag{10}$$

Substituting the following expression in Equation 10

$$\left[\delta\mathbf{K}(\mathbf{r},\delta\mathbf{r})\right]\left\{\mathbf{r}\right\} = \left[\mathbf{G}(\mathbf{r})\right]\left\{\delta\mathbf{r}\right\} + \left[\delta\mathbf{G}(\mathbf{r},\delta\mathbf{r})\right]\left[\delta\mathbf{r}\right] \tag{11}$$

and linearilizing the equation, Equation 10 reduces to the general incremental stiffness equation, namely

$$\left[\mathbf{K}(\mathbf{r}) + \mathbf{G}(\mathbf{r})\right]\left[\delta\mathbf{r}\right] = \left[\Delta\mathbf{R}\right] \tag{12}$$

where

$\mathbf{K}(\mathbf{r})$ is the standard elastic matrix calculated for the element geometry at deformation $\mathbf{r}$

$\mathbf{G}(\mathbf{r})$ is the so-called geometrical stiffness matrix that depends on the geometry and initial internal forces existing at deformation $\mathbf{r}$

Using Equation 12, the analysis of a nonlinear problem can be carried out in the conventional procedure established for the linear analysis above. For any arbitrary step **K** (r) and **G** (r) are calculated in the usual manner; that is, use is made of the geometry, material properties, and initial forces existing at the start of the step. Incremental loading then produces incremental displacements. Internal forces developed during the step are calculated from the incremental displacements in the conventional linear manner. Total values for displacements and internal forces are obtained by summing the incremental values. Note that **G** (O) = **O** because the geometrical stiffness matrix is proportional to the internal forces which are zero at the start of Step 1.

The piecewise linearization technique therefore applies to nonlinear problem efficiently because the step procedure corrects for deformation changes as loading takes place. At the same time the initial stress matrix is brought into the analysis. As in any approximate analysis of nonlinear problems, the accuracy of the determined displacements and internal forces increases as the number of steps increases. The concept of piecewise linearization in treating the large deflection problem by the direct stiffness method was first given by Turner, et al., in 1960 (Reference 11). Detailed analysis of trusses, beam structures, and plates using this procedure was given by (Reference 15). The necessary geometrical stiffness matrices and computing programs used in the analysis of the thin shells in this paper have been developed over a number of years at The Boeing Company by Turner, Martin, and others.

The application of the piecewise linearization technique to solve stability problems such as the shell stability considered in this paper can be carried out in a straightforward manner. The load is applied to the structure in increments and the total stiffness matrix is calculated and updated for each increment. Instability is indicated when the total load reaches its critical value making the determinant of the total stiffness matrix vanish. In some cases it may not be necessary to continue the piecewise linearization procedure to buckling. When the applied load on the structure is less than the critical buckling load, the value of the determinant $[K + G]$ will be positive and will tend toward zero as the applied load approaches the critical load. Consequently, an obvious scheme to predict the buckling load would be to plot $[K + G]$ versus the applied load, enabling the critical load to be approximated by extrapolation. Also another method that has been used to determine the critical buckling load instead of the continuation of the piecewise linearization technique to completion is the application of the Southwell's procedure. Using the deflection data generated at the end of each step a Southwell plot may be prepared and the critical load approximated. However, we found erratic results when we applied this method to very thin shallow shells.

SECTION III

SHELL ANALYSIS

SHALLOW SHELL ANALYSIS

Nineteen finite element models of shallow spherical shells were selected for analysis. These included variations of the shell thickness parameter, lambda, and variations in the relative node spacing or structural element size in the model. One of the models contained imperfections. All others had nodes defined in the perfect spherical surface. Plan views of the models are shown in Figure 3. The nodes are spaced uniformly around circles of latitude. The latitude circles are uniformly spaced along the plan view radii. The nodes are joined by flat triangular aluminum alloy 2024-T3 isotropic plates (References 32 and 33). Though shell elements would have been better than these plates, the necessary nonlinear stiffness matrices were not yet available for shell elements. Uniform pressure loads are replaced by equivalent concentrated loads at the nodes. The curved edge node freedoms are constrained to zero (clamped edges). The models are quadrants from circular models that are cut along symmetry lines. Symmetry conditions are enforced by constraints at nodes along these sides.

Figure 4 shows the imperfections in one of the models. These are scaled from those described analytically by Thurston and Penning (Reference 29) for one of Kaplan and Fung's test shells (Reference 23).

Figure 5 shows dimensions of the models, buckling strength of each model from differential equation solutions, load increment size, and buckling load for each of the analyses in this study.

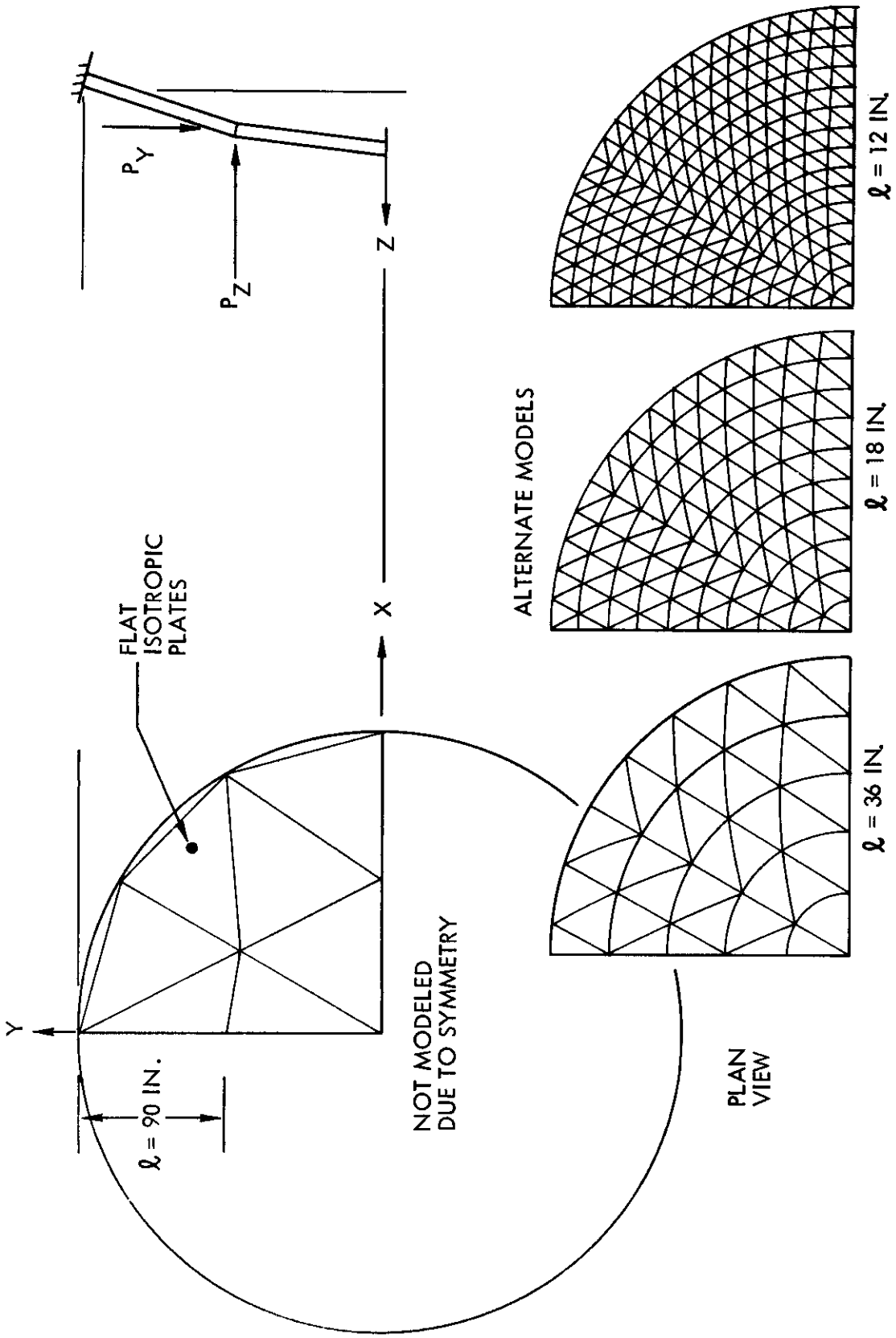

Figure 3. Model of Spherical Shell

r/a	0	.1	.2	.3	.4	.5	.6	.7	.8	.9	1.0
z_o/t	-.018	.030	.054	.044	.017	.023	.061	.063	-.028	-.165	-.023

Figure 4. Radial Distribution of Imperfection

ANALYSIS OF RESULTS

Figure 6 shows the ratio of finite element results to differential equation results plotted graphically against the ratio of load increment size to buckling load. The circles show the load that is unstable; the squares show the last load that yielded a stable deflection solution. Ignoring the very coarse models (dark points), the trend line was drawn so that no stable point was above it and no unstable point was below it.

Figure 7 shows the effect of node spacing on finite element results with the load increment size trend eliminated. Each solution was divided by the appropriate value from the trend line in Figure 6. From this figure it is concluded that node spacing should be no more than one-third the anticipated "half-wave buckle width." Coarser models apparently give erratic results. Finer models do not appear to improve the accuracy. The half-wave buckle width can be estimated from the formula in Timoshenko and Gere's book, "Theory of Elastic Stability" or from data in Figure 5.

STATISTICAL ANALYSIS OF DATA POINTS AVAILABLE

The deviations of the individual results from the trend line were treated statistically and the line of 1% probable exceedance was established with 95% confidence in Figure 8. The imperfect shell was not included in the statistical analysis but it is shown in Figure 8. The 1% exceedance line indicates the "overestimate factor" for finite element buckling analysis of uniformly loaded spherical shells. It had been expected to apply conservatively to any compound curved shell analysis; but the imperfect shell example, which represents only a small departure from uniform shperical shells, gave a solution that is above the exceedance line. Additional test correlation is apparently needed for shells with nonuniform pressure and nonspherical shape.

λ^*	NODE SPACING l^* IN	DIFF. EQU. BUCKLING NODE LOAD P_{cr} LB	INCREMENTAL NODE LOAD P LB	FINITE ELEMENT INSTABILITY NODE LOAD P_b LB	HALF-WAVE LENGTH OF BUCKLE L^* IN	IMPERFECTION
3.89	12	733,000	189,688	1,138,128	216	
3.89	18	1,650,000	511,500	2,557,000	216	
3.89	18	1,650,000	255,700	2,301,300	216	
3.89	18	1,650,000	170,470	2,045,640	216	
3.89	36	6,560,000	1,022,800	9,205,200	216	
3.89	36	6,560,000	204,560	6,955,000	216	
3.89	90	41,250,000	16,000,000	112,000,000	216	
6.10	18	363,000	78,100	468,000	90	
6.10	36	1,450,000	312,405	3,748,860	90	
6.10	36	1,450,000	62,481	1,562,025	90	
7.85	18	131,600	24,663	197,304	72	
7.85	18	95,542	24,662	172,634	72	See Figure 4
7.85	36	526,000	80,000	960,000	72	
7.85	36	526,000	19,730	789,222	72	
9.82	12	24,200	4,499	31,493	72	
9.82	18	54,500	10,123	80,984	72	
11.8	12	11,900	2,971	17,825	63	
11.8	18	26,700	4,864	38,912	63	
18	18	4,960	933	10,262	36	

* The spherical radii of all models were 540 inches. The plan view radii were 180 inches. L is measured half-wave length of buckle.

Figure 5. Dimensions and Buckling Strengths of Models

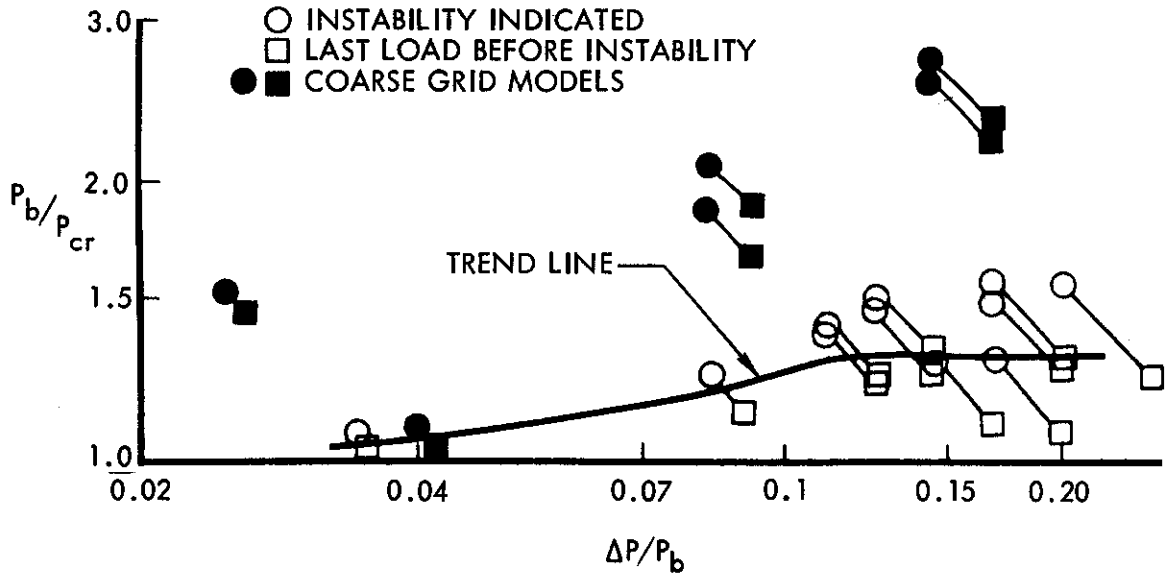

Figure 6. Effect of Load Increment Size

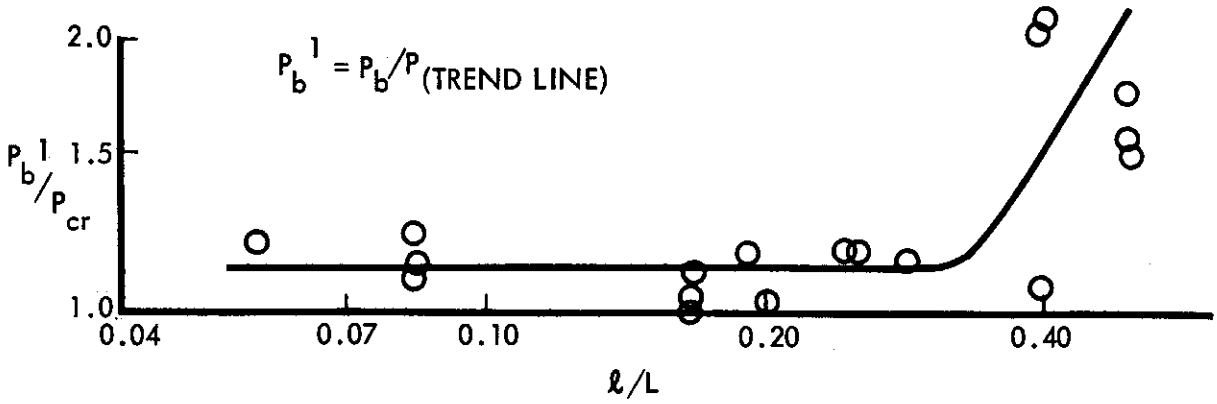

Figure 7. Effect of Node Spacing

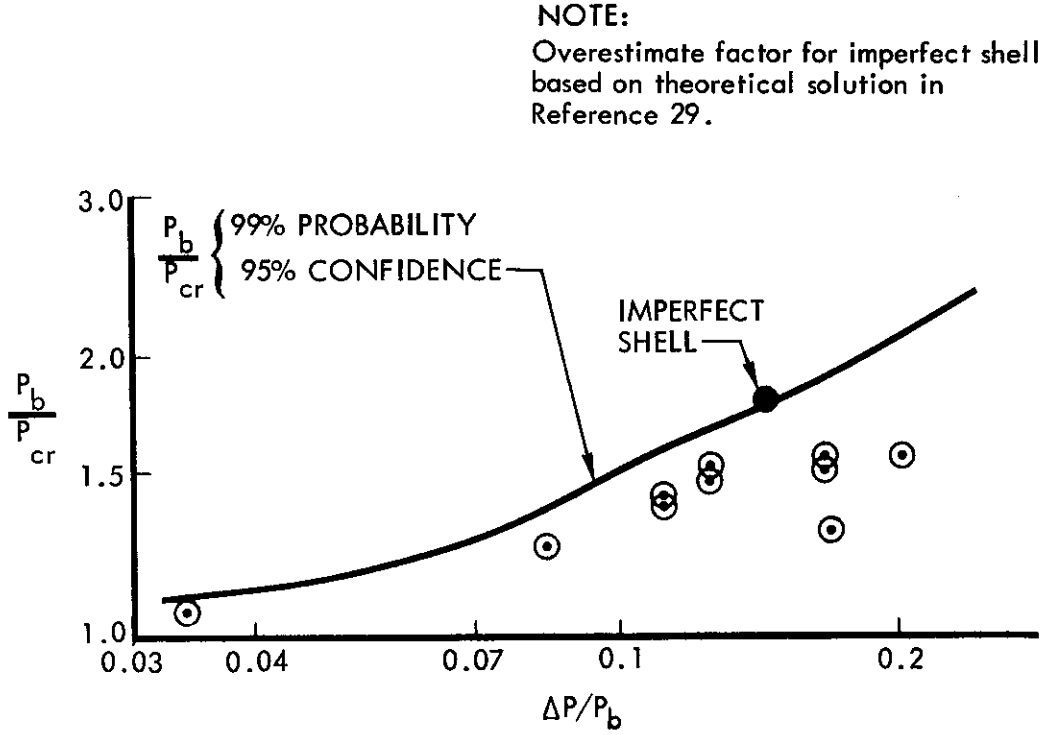

Figure 8. Statistical Overestimate Factor

EXAMPLE RADOME PROBLEM

Figure 9 shows a finite element model of the radome structure shown in Figure 1. The structure consists of two monocoque sandwich radomes plus a central support structure. The two radomes are modeled from flat triangular orthotropic plates with properties of a glass fiber honeycomb sandwich panel. In areas where the plates are nearly horizontal,beams are inserted in the model to constrain partially in-plane rotations and thereby condition the stiffness matrix. The central support structure contains aluminum bars, beams, shear webs, and surface panels sized to carry appropriate loads.

Figure 10 shows pressure distribution on the surface of the radome structure. The pressure at each node was taken from this figure and used to compute equivalent node loads.

Figure 11 shows deflections from the analysis. Each increment represents 100% of the pressure shown in Figure 10. Buckling was indicated in the fourth increment. Dividing the buckling load by the 1% exceedance value from Figure 8 gives a predicted strength of 165% of the pressures shown. Figure 8 is used pending developing of a similar chart for nonuniform shells.

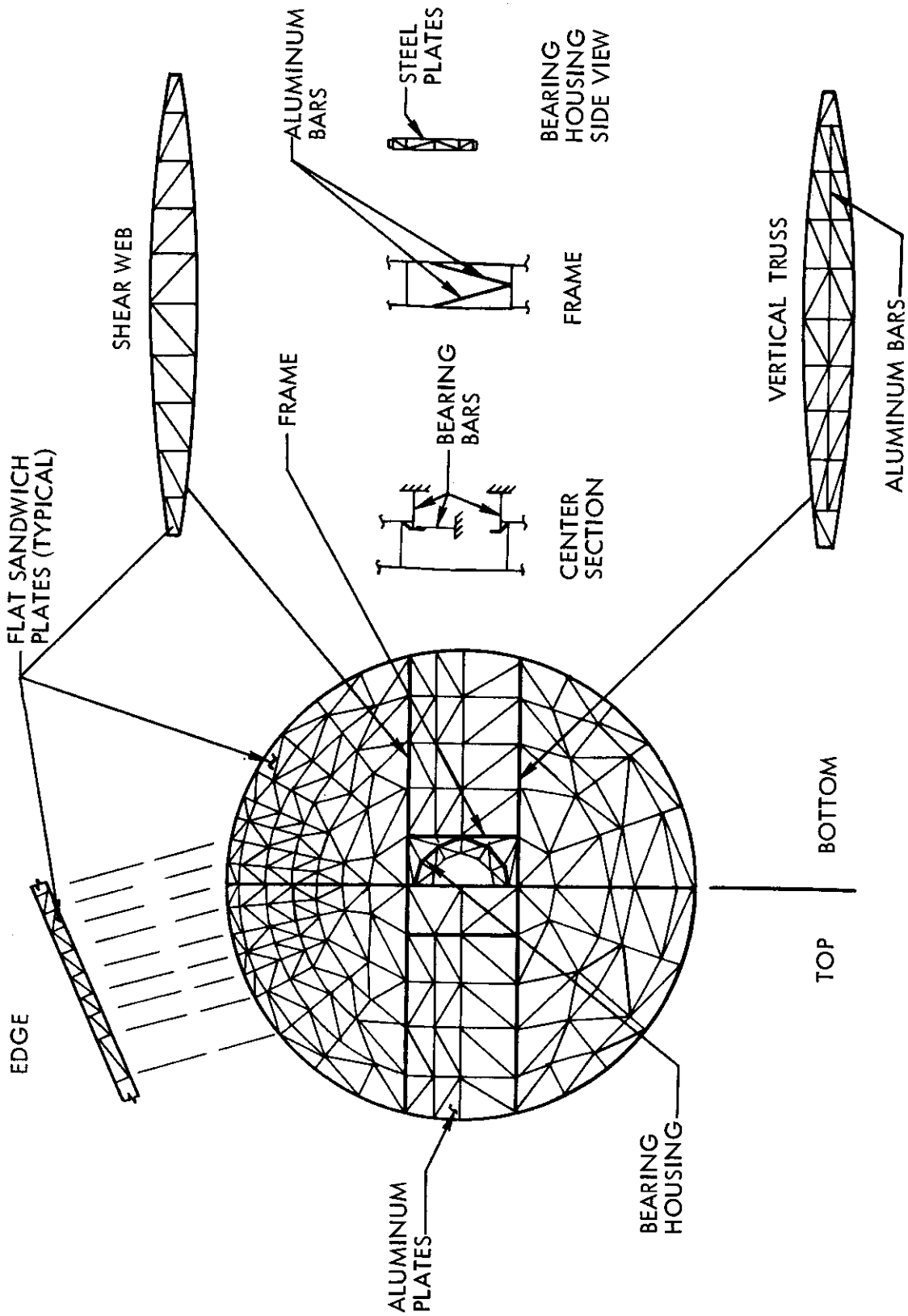

Figure 9. Model of Radome Structure

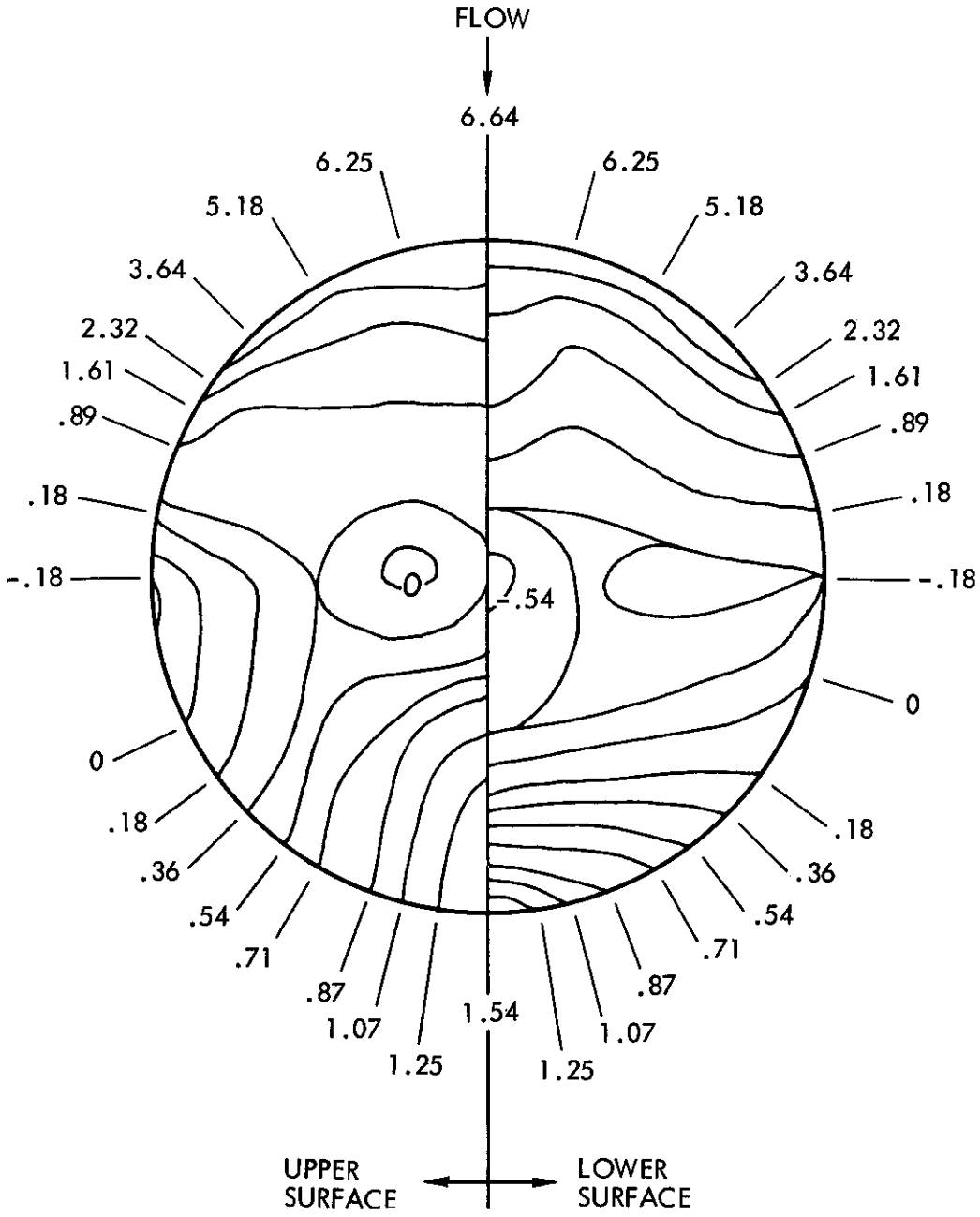

Figure 10. Differential Pressure Distribution (In PSI) on Radome

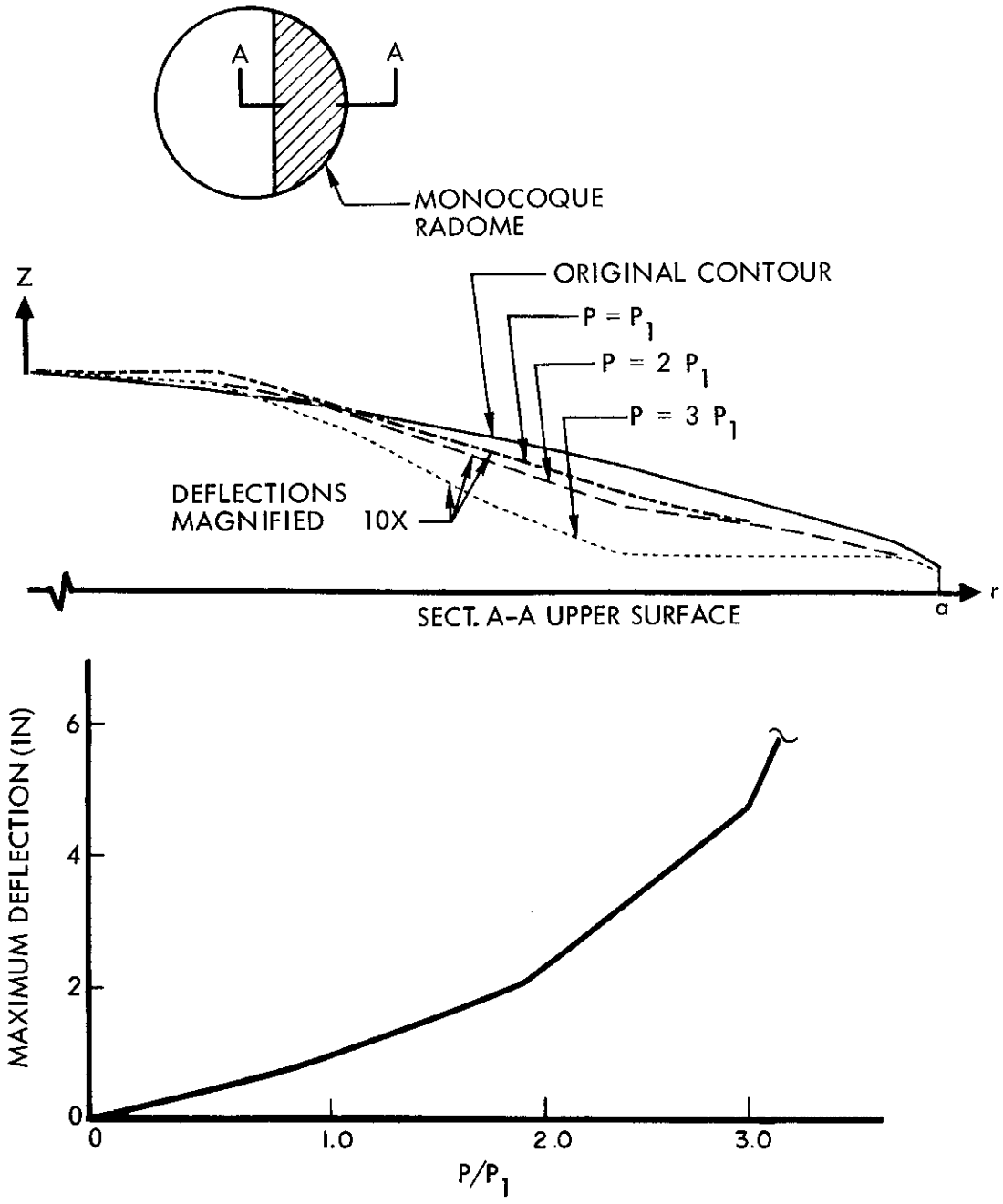

Figure 11. Thin Radome Deflection Data

Total thickness of the shell cross section in this radome was limited by electrical considerations. Consequently general instability of the shell was an unavoidable failure mode. It is noted that without such a constraint the designer, following normal design practice, would have chosen a thicker sandwich and attempted to avoid buckling. The job of the analyst would not be changed for the more conventional design because he still must show that instability doesn't occur below the design load and he must show any magnification of stress caused by approaching instability. Hence, the analysis technique we have used for buckling prediction is equally useful in checking a shell which is not expected to buckle.

Figure 12 shows deflections from another radome analysis with thinner sandwich faces and thicker sandwich core. Buckling as such did not occur, but stress in the sandwich faces exceeded the allowable value. Local failure of the faces would no doubt have caused a collapse of the radome. Because there was no buckling load it was not possible to correct this analysis from Figure 8 directly. An indirect method was devised and it will be described here because many practical shell problems may have similar failure modes. A similar load-deflection curve was produced in a very thick spherical cap (lambda = 3) and would be expected in thick sandwich with thin faces.

Figure 13 shows a deflection magnification factor as a function of the ratio of load to buckling load. The points in the figure were taken from two of the shallow spherical shell finite element analyses. The magnification factor is the ratio of total deflection to the deflection that would have been predicted by a linear analysis. The curve in the figure shows

$$\delta_{F.E.} = \frac{\delta_0}{(1 - P/P_b)^{.312}} \tag{13}$$

It is assumed that an exact solution will yield a similar equation

$$\delta = \frac{\delta_0}{(1 - P/P_{cr})^{.312}} \tag{14}$$

Hence

$$\delta = \delta_{F.E.} \frac{(1 - P/P_b)^{.312}}{\left(1 - \frac{P}{P_b} \quad \frac{P_b}{P_{cr}}\right)^{.312}} \tag{15}$$

The ratio P_b/P_{cr} can be taken from Figure 8.

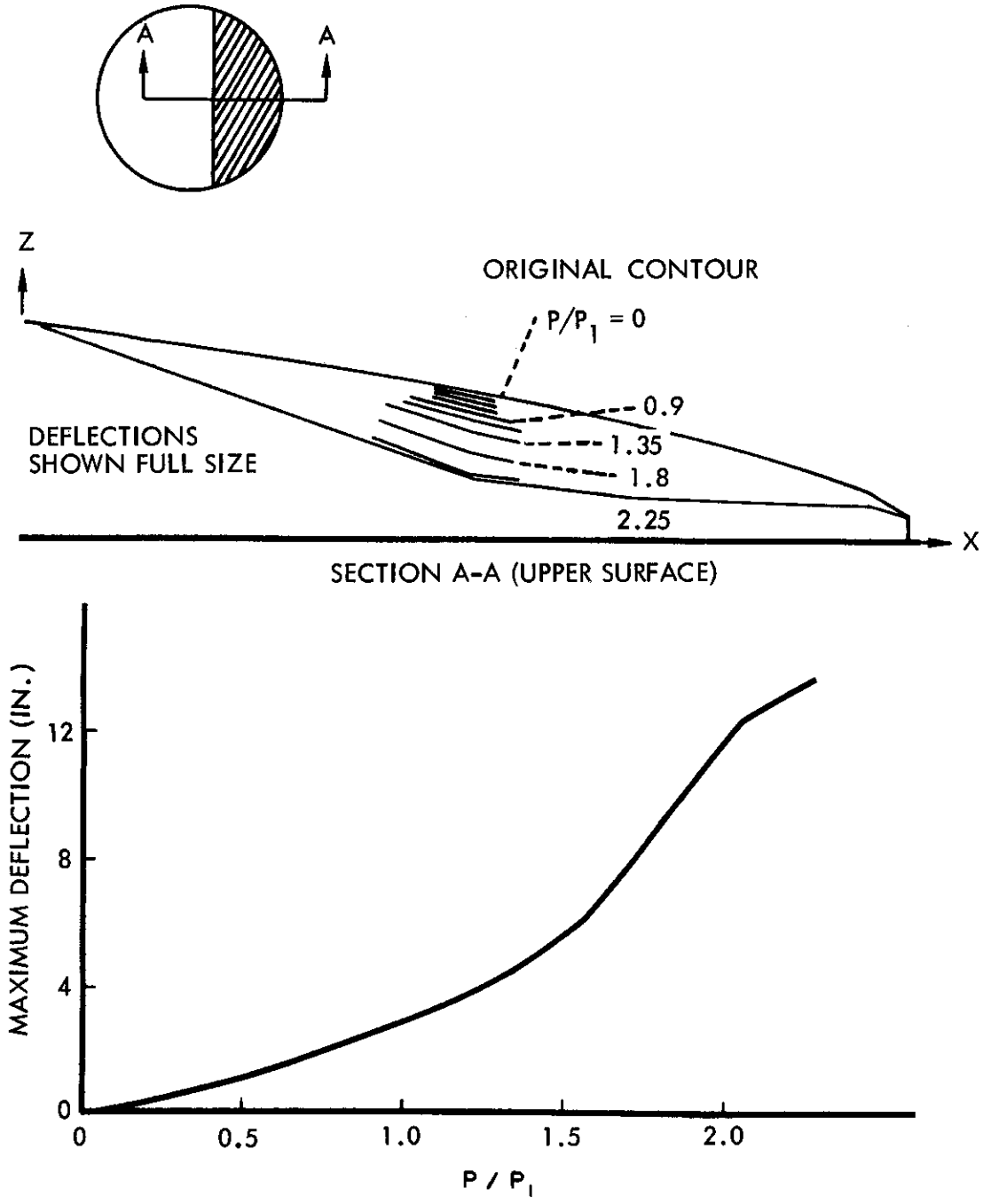

Figure 12. Thick Radome Deflection Data

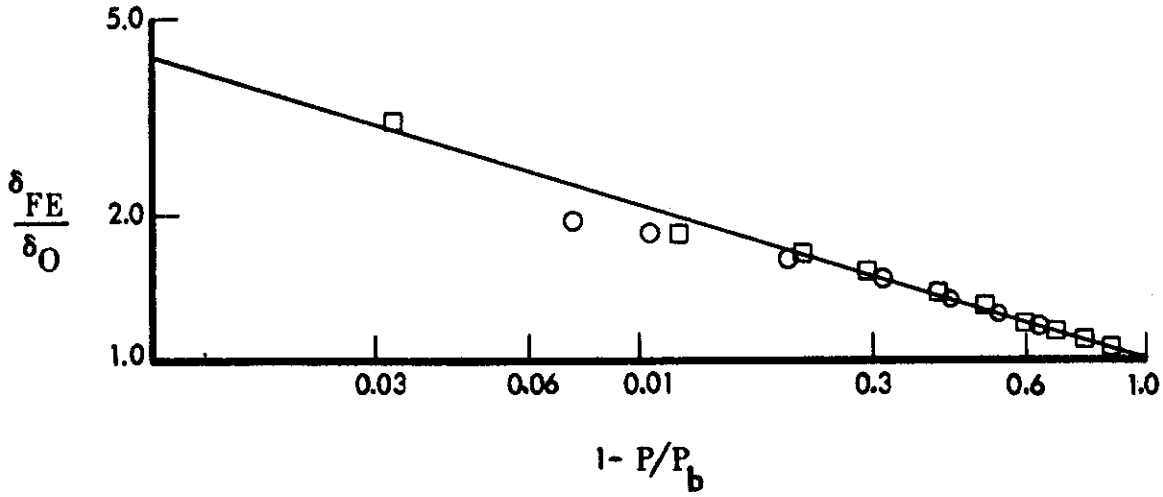

Figure 13. Deflection Magnification Factors

A pseudo-buckling load is obtained by solving Equation 13 for P_b at one of the load levels in the steep part of the load-deflection curve.

$$P = P\left[1 - \left(\frac{\delta_{FE}}{\delta_O}\right)^{3.2}\right] \tag{16}$$

The deflections are then indicated by applying Equations 14 and 15 to the finite element deflections. Stresses can be approximated from the stress-deflection data in the finite element solution.

SECTION IV

CONCLUSION

The use of a practical finite element analysis method to predict buckling of doubly curved shells has been demonstrated. Results of several such analyses have been compared to differential equation solutions which are considered to be exact buckling predictions. As expected, the raw finite element results tend to be unconservative. However, the amount of unconservatism can be correlated with analysis modeling parameters so that an appropriate overestimate factor can be determined for a given analysis. The overestimate factor for uniformly loaded shallow spherical shell has been determined statistically.

Use of the same method has been demonstrated on an imperfect shallow spherical shell and a more complicated shell problem. The overestimate factors for such problems have not yet been established. The flexibility of the analysis method in dealing with shells that deflect nonlinearly with or without ultimate instability can be seen.

Additional work is needed to determine overestimate factors for other shell buckling problems. Development of nonlinear matrices for shell elements is also needed so as to improve analysis accuracy and thereby to reduce overestimate factors.

SECTION V

REFERENCES

1. Reissner, H., Spannungen in Kugelschalen (Kuppeln), Festschrift, H. Muler-Breslau, pp. 181-193, 1912.

2. Van der Neut, A., Dissertation, Delft, 1932.

3. Timoshenko, S., Theory of Elastic Stability, McGraw-Hill, pp. 439-490, 1936.

4. Gerard, G., Handbook of Structural Stability, NACA TN-3781, 3782, 3783, 3784, 3785, and 3786, August 1957.

5. NASA TND-1510, Collected Papers on Instability of Shell Structures, Langley Research Center, 1962.

6. Von Kármán, T., and H. Tsien, "The Buckling of Spherical Shells by External Pressure," Journal of the Aeronautical Sciences, pp. 43-50, December 1939.

7. Huang, Hai-chien, "Unsymmetrical Buckling of Thin Shallow Spherical Shells," Journal of Applied Mechanics, pp. 447-456, September 1964.

8. Argyris, J. H., and S. Kelsey, "Energy Theorems and Structural Analysis," Aircraft Engineering, (a series) October 1954, November 1954, February 1955, March 1955, April 1955, and May 1955 (Reprinted by Butterworths, London, 1960).

9. Turner, M. J., R. W. Clough, H. C. Martin, and L. J. Topp, "Stiffness and Deflection Analysis of Complex Structures," Journal of the Aeronautical Sciences, pp. 805-823, 854, September 1956.

10. Denke, P. H., Martix Structural Analysis, Paper presented the 2nd National Conference of Applied Mechanics, Ann Arbor, Michigan, 1954.

11. Turner, M. J., E. H. Dill, H. C. Martin, and M. J. Melosh, "Large Deflections of Structures Subjected to Heating and External Loads," Journal of the Aero/Space Sciences, pp. 97-107, 127, February 1960.

12. Gallagher, R. H., J. Padlog, and R. D. Huff, Thermal Stress Determination Techniques for Supersonic Transport Aircraft Structures, Part III, Computer Programs for Beam, Plate and Cylindrical Shell Analysis, ASD-TDR-63-783, Air Force Systems Command, January 1964.

13. Hartz, B. J., "Matrix Formulation of Structural Stability Problems," Journal of Structural Division, Proceedings of ASCE, pp. 141-157, December 1965.

14. Hartz, B. J., and K. K. Kapure, "Stability of Plates Using the Finite Element Method," Journal of the Engineering Mechanics Division Proceedings of ASCE, pp. 177-195, April 1966.

15. Martin, H. C., Large Deflection and Stability Analysis by the Direct Stiffness Method, JPL Technical Report No. 32-931, California Institute of Technology, August 1966.

16. Gallagher, R. H., R. A. Gellatly, J. Padlog, and H. M. Mallett, "A Discrete Element Procedure for Thin-Shell Instability Analysis," AIAA Journal, pp. 138-145, January 1967.

17. Budiansky, B., "Buckling of Clamped Spherical Shells, Proceedings of the Symposium on the Theory of Thin Elastic Shells," North Holland Publishing Company, pp. 64-94, 1950.

18. Weinitschke, H. J., "On the Nonlinear Theory of Shallow Spherical Shells," Journal of the Society for Industrial and Applied Mathematics, Vol. 6, p. 209, 1958.

19. Thurston, G. A., "A Numerical Solution of the Nonlinear Equations for Axisymmetric Bending of Shallow Spherical Shells," Journal of Applied Mechanics, Vol. 28, pp. 557-568, 1961.

20. Feodosiev, V. I., "Calculations of Thin Clicking Membranes," Prikladnaia Matematika i Mekhanika, Vol. X, p. 295, 1946.

21. Chen, W. L., Effect of Geometrical Imperfections on the Elastic Buckling of Shallow Spherical Shells, Sc. D Thesis, Department of Civil and Sanitary Engineering, Massachusetts Institute of Technology, January 1959.

22. Archer, R. R., "Stability Limits for a Clamped Spherical Shell Segment Under Uniform Pressure," Quarterly of Applied Mathematics, p. 355, January 1958.

23. Kaplan, A., and Fung, Y. C., A Nonlinear Theory of Bending and Buckling of Thin Elastic Shallow Spherical Shells, NACA TN 3212, 1954.

24. Reiss, E. L., H. J. Greenberg, and H. B. Keller, "Nonlinear Deflections of Shallow Spherical Shells," Journal of the Aeronautical Sciences, p. 533, July 1957.

25. Gjelsuik, A., and Bodner, S. R., The Non-symmetrical Snap Buckling of the Clamped Spherical Cap, Technical Report No. 30, Engineering Division, Brown University, March 1962.

26. Parmerter, R. D., and Fung, Y. C., On the Influence of Nonsymmetrical Modes on the Buckling of Shallow Spherical Shells Under Uniform Pressure, NASA TND-1510, p. 491, 1962.

27. Parmerter, R. D., The Buckling of Shallow Spherical Shells Under Uniform Pressure, Aeroelasticity and Structural Dynamics Report No. SM 63-53, Graduate Aeronautical Laboratories, California Institute of Technology, November 1963.

28. Weinitschke, H. J., Assymmetrical Buckling of Clamped Spherical Shells, NASA TND-1510, 1962, p. 481.

29. Thurston, G. A., and Penning, F. A., "Effect of Axisymmetric Imperfections on the Buckling of Spherical Caps Under Uniform Pressure," AIAA Journal, pp. 319-327, February 1966.

30. Turner, M. J., H. C. Martin, and R. C. Weikel, Further Development and Applications of the Stiffness Method, presented at a meeting of the AGARD Structures and Material Panel, Paris, France, July 6, 1962.

31. Gallagher, R. H., and R. J. Padlog, "Discrete Element Approach to Structural Instability Analysis", AIAA Journal, June, 1963, pp. 1437-1439.

32. Martin, H. C., Stiffness Matrix for a Triangular Sandwich Element in Bending," JPL Technical Report No. 32-1158, California Institute of Technology, October, 1967.

33. Martin, H. C., On The Derivation of Stiffness Matrices For the Analysis of Large Deflection and Stability Problems, Proceedings of the Conference on Matrix Methods in Structural Mechanics held at Wright-Patterson Air Force Base, Ohio (AFFDL-TR-66-80), October, 1965.